

M. COTTE<sup>1,3,✉</sup>  
E. CHECROUN<sup>2</sup>  
J. SUSINI<sup>3</sup>  
P. WALTER<sup>1</sup>

# Micro-analytical study of interactions between oil and lead compounds in paintings

<sup>1</sup> Centre de Recherche et de Restauration des Musées de France (C2RMF), UMR 171 CNRS, Palais du Louvre, Porte des Lions, 14 quai F. Mitterrand, 75001 Paris, France

<sup>2</sup> Institut National du Patrimoine, 150 avenue du Président Wilson, 93210 La Plaine Saint Denis, France

<sup>3</sup> European Synchrotron Radiation Facility, BP 220, 38043 Grenoble Cedex, France

Received: 1 October 2006 / Accepted: 25 June 2007

Published online: 15 August 2007 • © Springer-Verlag 2007

**ABSTRACT** Oil paintings are complex hybrid materials, made of organic binders associated with inorganic minerals, susceptible to evolving over centuries. In particular, interactions of oil with lead compounds may give rise to the formation of lead soap aggregates, so-called protrusions. This phenomenon is studied here via X-ray and FTIR micro-analysis of an ancient painting dated from 1610. In complement, the synthesis of modern preparations, reconstructed from ancient recipes was assessed. Molecular and atomic images are obtained by combining synchrotron-based FTIR and X-ray fluorescence microscopies. Protrusions are identified in both ancient and modern samples, more particularly, in the ground layer of the paintings, below the colored layer. These observations imply that lead oxide, introduced as a siccative and not as a pigment, may be the element mainly responsible for the protrusions formation, and that this degradation may appear very rapidly on paintings.

PACS 87.64.Je; 82.80.Gk; 82.40.Bj

## 1 Introduction

The question of long-term interactions in cultural heritage objects is an inescapable problem. Even though the technical capabilities of instruments increase in terms of sensitivity, non-destructivity or lateral resolution, a remaining crucial issue is the data interpretation when dealing with long time-scale: was the sample as it is now? How relevant is the chemical information obtained on centuries old objects? What about long-term evolutions?

This article deals with the specific case of the interactions of oil and lead compounds (salts and oxides). Such mixtures were used both in painting (lead was employed as a pigment or as a siccative, and mixed with oil) and also in cosmetics (such as lead plasters and unguents). Organic matter is known to suffer from alteration phenomena, among which reactions with lead oxides that may end in oil saponification. The resulting lead soaps have already been observed in ancient materials. Their presence in cosmetics was the subject of two previous articles [1, 2]. Here, some light is shed on oil saponification in paintings. Lead soaps are a puzzling problem for conser-

vators because they can appear as local aggregates, so-called protrusions. These spots may be white or orange, from tens of micrometers up to millimeters in size. The critical point is their local organization which affects the plasticity of the matter, resulting in painting cracking (Fig. 1). The appearance of these protrusions is not perfectly understood. It is commonly assumed that it comes from a long interaction between oil and lead pigments [3–5]. This work aims to better understand the formation of these lead soap aggregates.

The approach proposed here is rather transversal. In terms of the sample: ancient objects, ancient texts and modern reconstruction are studied as well. In terms of analytical chemistry: both organic and mineral components are analyzed on the atomic and molecular levels, thanks to the combination of micro X-ray fluorescence ( $\mu$ -XRF) and Fourier-transform infrared (FTIR) microscopies. In terms of scale: a microscopic approach is favored here, in particular imaging methods that enable resolving of the elemental and molecular heterogeneity. It completes a macroscopic approach which was previously developed on the saponification kinetics of oil-lead compound mixtures [2]. The lateral resolution of images was improved thanks to the use of synchrotron radiation (SR).

The starting point of this study was the chemical micro-analysis of orange aggregates existing on an anonymous portrait dating from 1610. Macroscopic observations suggested that some lead soap protrusions were present, which was confirmed by both FTIR and XRF microscopies. The comparison of chemical information obtained on the ancient painting with contemporaneous painting recipes reinforces the hypothesis that the painting was made with a lead-medium ground layer mixed with some ochre. This preparation was reconstructed in order to evaluate its properties and its stability. Two sets of model samples were then prepared: a painting facsimile and different combinations of lead-medium mixed with pigments.

## 2 Samples and methods

### 2.1 Samples

**2.1.1 The ancient painting.** The oil painting studied here is an anonymous portrait made on canvas, dating from 1610, measuring  $50 \times 65 \text{ cm}^2$  and conserved in the Musée du Chatillonais, France (N° inv. 15) (Fig. 1). Its author is unknown but it is stylistically attributed to a Northern school.

✉ Fax: +33-1-40205759, E-mail: marine.cotte@culture.gouv.fr



**FIGURE 1** The anonymous portrait, dated from 1610, oil on canvas, Musée du Chatillonnais, France (left). (Picture taken by Gyslain Vanneste, Inp.) Zoom on some protrusions (right)

**2.1.2 Preparation of cross-sections of the fragments from the ancient painting.** FTIR microscopy can be performed in two main configurations: transmission and reflection. The spectral quality is generally much higher working with the transmission mode, but concomitantly it requires a more arduous sample preparation. Several methods have been proposed to tackle this problem in the case of painting samples. Most of them are based on the use of thin cuts of polymer blocks, obtained with a microtome [6–9]. The major inconvenience is the possible diffusion and interference of the embedding medium inside the sample. An encapsulating method was proposed to prevent this infiltration [7]. An alternative to these methods relies on the use of an inorganic substrate ( $\text{BaF}_2$ ,  $\text{AgCl}$ ,  $\text{KBr}$ ) which will be transparent in the considered infrared domain [7, 9]. This substrate is powdered and then placed in a pellet die. The sample is put at the center of the die and covered with additional substrate. The set is pressed into a transparent window. Afterward, the pellet is polished on both sides in order to get a thin cross-section of the sample. A complete description of the method can be found in [9].

Eight pellets were prepared in this way, using  $\text{KBr}$  as the medium, with samples taken on protrusion spots, on different locations of the portrait. This preparation method requires patience and perseverance as the final thickening can unfortunately end into the complete loss of the sample.

**2.1.3 Synthesis of model mixtures and facsimile.** The preparation of model mixtures of oil and lead compounds (lead-medium) is described elsewhere [2]. In brief, oil and lead compounds (salts or oxides) are mixed, with or without water, and heated. The making up of a painting lead-medium was performed following a recipe given in 1633 by Sir Theodore Turquet de Mayerne [2].

The preparation of the facsimile painting was inspired by the chemical information obtained from an analysis of the ancient painting (see below). Considering the technical

problems encountered for the preparation of cross-sections using the  $\text{KBr}$  pellet method, cross-sections of the facsimile were obtained differently. Samples of about  $6 \text{ mm}^3$  were taken and wrapped into an aluminum foil. The set was placed in an embedding resin (Leica Historesin) and cuts of  $5 \mu\text{m}$  were obtained with a microtome (2055 Autocut, Jung, Leica) equipped with a diamond knife. This technique was facilitated by the relative flexibility of the three-month-old painting. The aluminum foil is a good barrier against resin diffusion inside the sample. This method is preferential to the  $\text{KBr}$  method as the quality of spectra is much higher and as it avoids possible distortion of the beam within the  $\text{KBr}$  under layer.

## 2.2 Methods

**2.2.1 FTIR microscopy.** FTIR microscopy was performed on the ID21-infrared end station, at the ESRF (France) [10]. The instrument is a Nexus spectrometer coupled with a confocal continuum microscope from Nicolet. The advantage of synchrotron radiation versus a thermal source is the high brightness of the beam, which results from the natural low divergence and the use of focusing mirrors. Namely, even if integrated over the whole space, the total number of photons emitted by the SR is lower than with the global source, when working with small apertures, e.g. below  $15 \times 15 \mu\text{m}^2$ , the signal obtained with the SR is far much intense than with the global. Depending on the experimental conditions required, the source used is either the internal global light, or the synchrotron emission. More precisely, the global is more adapted to study large regions with a low resolution ( $25 \times 25 \mu\text{m}^2$ ), whereas SR is needed to get detailed acquisitions, with a higher resolution ( $8 \times 8 \mu\text{m}^2$ ). The set up can be easily switched from one mode to another. The step size was adapted to the beam size. FTIR spectra are made of an average of 20 scans for acquisition with the SR and a minimum of 64 scans with the global. The spectral resolution was set to  $8 \text{ cm}^{-1}$  in both cases.

**2.2.2 X-ray micro-fluorescence.** Elemental maps were obtained using the ID21 scanning X-ray microscope, at the ESRF (France). Briefly, the fluorescence excitation is stimulated with a highly monochromatic beam by means of a fixed-exit double crystal  $\text{Si}(111)$  monochromator, with a tunable energy ranging from 2.1 to 7.2 keV. Fresnel zone plates are used as focusing optics to generate a sub-micrometer X-ray probe. The micro-fluorescence signal is collected in the horizontal plane perpendicular to the incident beam direction by using a HPGe solid-state energy-dispersive detector. The detailed setup is described elsewhere [11].

Acquisitions were first obtained with an exciting energy of 7.2 keV (step size of  $5 \mu\text{m}$  in both directions) to show most of the elements ( $K$ -lines of Na to Fe,  $L$ -lines of Br and  $M$ -lines of Pb). The fluorescence of lead was overexcited by working just above the  $M_{IV}$  edge (2.7 keV, step size of  $2.5 \mu\text{m}$  in both directions). As shown in Fig. 4a, spectra analysis is difficult due to the significant overlap of the fluorescence lines of atoms of interest. In particular Si, Pb and S do interfere. The spectra fitting was performed by using dedicated software, PyMCA. This program implements a Levenberg–Marquardt

algorithm to fit the spectra with constraints on the fitting parameters (detector characteristics, detection geometry, matrix composition, exciting energy ...). A more detailed description of this code is found in reference [12].

Finally, XANES spectra at Pb  $M_V$  and  $M_{IV}$  edges were collected in fluorescence and transmission modes from 2.45 to 2.68 keV, with a 0.25 eV-step.

### 3 Results and discussion

#### 3.1 Analysis of ancient samples

Eight fragments of protrusions taken on the ancient painting were studied. They exhibit similar characteristics. Results and discussion are given on a particular cross-section, whose picture is shown in Fig. 2VL. The painting is made of two main layers: an ochre ground layer, about 350  $\mu\text{m}$ -thick, covered with a brown colored layer, around 70  $\mu\text{m}$ -thick. In fact, the superficial layer may be composed of different sub-layers of various colors as well as a varnish layer. Few efforts were made to improve the distinction of these sub-structures as the main objective of this work was focused on the protrusion phenomenon, which mainly occurs in the ground layer (Fig. 1).

FTIR spectra acquired in different locations confirm that the sample is a complex mixture of both mineral and organic phases (Fig. 2, spectrum (1) to (4)). Spectra are plotted with common absorption scale and offset for convenient reading. Grey rectangles indicate characteristic bands of our interest. Comparisons with references enable the identification of clays, more precisely kaolinite ( $\text{Al}_2\text{Si}_2\text{O}_5(\text{OH})_4$ ), referenced as “k” (Fig. 2, spectrum (4)) and quartz ( $\text{SiO}_2$ ), referenced

as “q” (Fig. 2, spectrum (3)). Characteristic absorption bands were used to obtain the chemical maps of these two minerals (Fig. 2k and q, respectively). Both are present in the ground layer, the kaolinite being well dispersed while quartz appears as transparent 50  $\mu\text{m}$ -diameter particles, visible on Fig. 2VL. Some carbonates, referenced as “c”, are also identified thanks to the large band around 1405  $\text{cm}^{-1}$  (Fig. 2, spectrum (2)). Even if the signal may saturate in this wavenumbers domain, the chemical map shows that carbonates are more concentrated in the superficial colored layer (Fig. 2c). The additional presence of a fine O–H stretching band at 3535  $\text{cm}^{-1}$  is in favor of the identification of hydrocerussite ( $(\text{PbCO}_3)_2 \cdot \text{Pb}(\text{OH})_2$ ), a compound currently used in painting when associated with cerussite ( $(\text{PbCO}_3)_2$ ) and called lead white (cf. reference spectrum Fig. 7, spectrum (3)) [13].

Regarding the organic compounds, long fatty chains, referenced as “f”, are easily identified thanks to the presence of a characteristic bands from 2800 to 3000  $\text{cm}^{-1}$  ( $\text{CH}_x$  stretching). They can be found in both ground and painted layers (Fig. 2f). The high intensity of the signal in the center of the map could be due not only to a higher concentration but also to a higher absorption coefficient of species present in this area (see Fig. 2, spectrum (1) and below). No unsaturation was detected ( $\text{C}=\text{C}-\text{H}$  stretching at 3009  $\text{cm}^{-1}$ ), which does not mean that they were not originally present in oil. Such double bonds are very sensitive to degradation and disappear rapidly, for example during oil drying [14].

The chemical map, Fig. 2u, represents the absorbance integrated from 1805 to 1672  $\text{cm}^{-1}$ , which covers the contribution of both ester and acid groups. These two forms exhibit characteristic  $\text{C}=\text{O}$  stretching at around 1737 and 1712  $\text{cm}^{-1}$

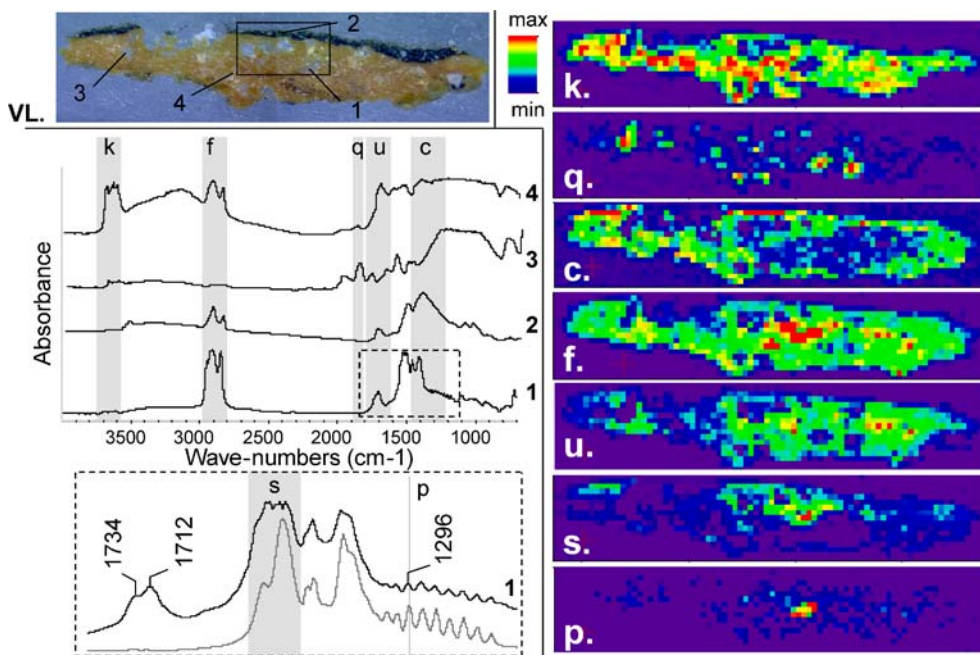


**FIGURE 2** Analysis by FTIR microscopy of a protrusion fragment of the painting: visible light image of the polished cross-section (VL). Spectra acquired at different locations, common absorption scale with an artificial offset. In the inset, a zoom from 1800 to 1150  $\text{cm}^{-1}$  of spectrum (1) (black), compared with the reference spectrum of lead palmitate (grey). Chemical maps of kaolinite (intensity from 3747 to 3562  $\text{cm}^{-1}$ ) (k), quartz (intensity from 1930 to 1836  $\text{cm}^{-1}$ ) (q), carbonates (intensity from 1481 to 1254  $\text{cm}^{-1}$ ) (c), fatty chains  $\text{CH}_x$  (intensity from 3041 to 2780  $\text{cm}^{-1}$ ) (f), unsaponified groups (acids and esters, intensity from 1805 to 1672  $\text{cm}^{-1}$ ) (u), saponified groups (carboxylates, intensity from 1594 to 1485  $\text{cm}^{-1}$ ) (s), palmitic chains (intensity at 1295  $\text{cm}^{-1}$ , with a baseline from 1305 to 1285  $\text{cm}^{-1}$ ) (p). Map size: 2.05  $\times$  0.4  $\text{mm}^2$ . The black rectangle represents the area analyzed in Figs. 3 and 4

respectively (cf. inset Fig. 2). Their distribution follows more or less the map of fatty chains.

Additionally, lead carboxylate groups, referenced as “s” for soaps, are evidenced by the large C=O asymmetric stretching vibration, around  $1520\text{ cm}^{-1}$ . They are present in both ground and painted layer, with an interesting high spot, of about  $60\text{ }\mu\text{m}$ -diameter, in the center of the map (Fig. 2s). This region has a visible aspect typical of all the protrusions studied, with a white matrix mixed with small orange particles. In this area, spectra exhibit a particular shape, as imaged in the inset (Fig. 2). The set of small narrow bands between  $1350$  and  $1100\text{ cm}^{-1}$  is characteristic of palmitic chain (referenced as “p”) [1, 15, 16]. The intensity map of one of these bands shows that this precise signal is principally observed in a central spot of about  $60\text{ }\mu\text{m}$ -diameter (Fig. 2p) corresponding to high amounts of lead soap (Fig. 2s).

A more detailed analysis of this area was conducted thanks to the use of the bright SR beam. The beam spot was reduced from  $25 \times 25$  down to  $8 \times 8\text{ }\mu\text{m}^2$ , the step size from  $25$  to  $5\text{ }\mu\text{m}$  in both directions and the number of scans per point from 128 to 20. The map is indicated with the black rectangle in Fig. 2VL. Raw images (unsmoothed) are shown in Fig. 3. They offer a more precise vision of the information given previously: carbonates on the surface (Fig. 3c), large particles of quartz (Fig. 3q) surrounded by a mixture of kaolinite (Fig. 3k), fat (Fig. 3f), partially saponified carboxylic groups (Fig. 3u and s). Figure 3s and p highlight the spot of lead palmitates.

In addition, elemental maps were obtained on exactly the same area of interest by micro X-ray fluorescence (Fig. 4b). The colored layer is mainly made of lead. In the ground layer, lead, silicon and iron are dispersed around grains of silicon and lead. These maps corroborate the interpretation of FTIR spectra, in particular, the identification of lead carbonates (in the colored layer, cf. Fig. 3c), lead carboxylates (dispersed in the ground layer and concentrated in some high spots, cf. Fig. 3s), kaolinite (dispersed in the ground layer, cf. Fig. 3k) as well as particles of quartz in the ground layer (cf. Fig. 3q). The map of bromine is given for information, and shows that the cross-sections prepared as described here are compatible for both FTIR and X-ray microscopies, i.e. that the fluorescence of bromine (originated from KBr substrate) is a tolerable artifact. Its main inconvenient is that it highly interferes with aluminum fluorescence thus preventing its clear detection.

The misfitting of soaps and lead images on the left-bottom corner of the map (Figs. 3s and 4bPb) is due to a complete absorption of the infrared beam, below  $1500\text{ cm}^{-1}$ . Conversely to micro X-ray fluorescence, FTIR spectra are highly affected by the sample thickness as measurements are done in transmission. This problem is due to the sample preparation which hardly provides a constant thickness over the full analyzed area, in contrast to microtome. Because of this complete absorption, FTIR spectra could not be fully exploited in this area of the map.

In order to get better insight into the identification of lead salts and oxides used in the preparation of the ground layer (in particular, it is relevant to differentiate the two lead oxides litharge (PbO) and minium ( $\text{Pb}_3\text{O}_4$ ), both currently used in paintings), lead-XANES was performed at the  $M_{IV}$

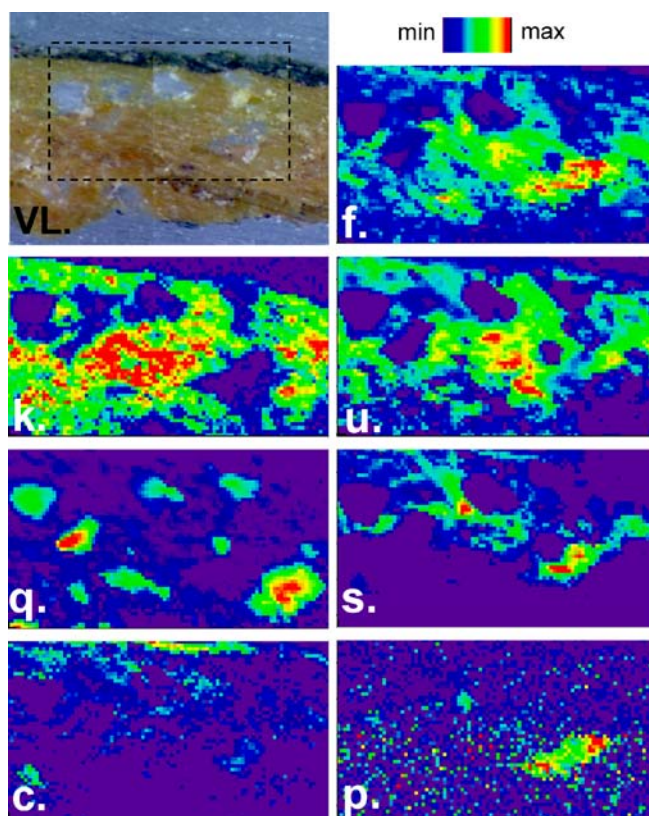


**FIGURE 3** Analysis by SR-FTIR microscopy of a protrusion fragment: visible light image of the polished cross-section (VL). Chemical map of kaolinite (k), quartz (q), carbonates (c), fatty chains  $\text{CH}_x$  (f), unsaponified groups (acids and esters) (u), carboxylates (s), palmitic chains (p). See Fig. 2 for details on data processing and for a wider view of the sample. Map size:  $450 \times 250\text{ }\mu\text{m}^2$

and  $M_V$ -edges ( $2.586$  and  $2.484\text{ keV}$  respectively). Spectra of references were first acquired on various lead salts and oxides (minium ( $\text{Pb}_3\text{O}_4$ ), lead-tin yellow ( $\text{Pb}_2\text{SnO}_4$ ), lead oxide (PbO) (commercial mixture of the two phases litharge and massicot), cerussite ( $\text{PbCO}_3$ ), phosgenite ( $\text{Pb}_2\text{CO}_3\text{Cl}_2$ ), acetate ( $\text{Pb}(\text{C}_2\text{H}_3\text{O}_2)_2 \cdot 3\text{H}_2\text{O}$ ), chloride ( $\text{PbCl}_2$ ), laurionite ( $\text{PbOHCl}$ ), palmitate ( $\text{Pb}(\text{C}_{16}\text{H}_{30}\text{O}_2)_2$ ), lead white (commercial mixture of cerussite and hydrocerussite), nitrate ( $\text{Pb}(\text{NO}_3)_2$ ), galena (PbS) and anglesite ( $\text{PbSO}_4$ ) (Fig. 5c–o). Features at the  $M_{IV}$ -edge ( $3d_{3/2}$ ) ( $2.6\text{ keV}$ ) are more or less homothetic of the features at the  $M_V$ -edge ( $3d_{5/2}$ ) ( $2.5\text{ keV}$ ). Even if weaker, they are important in the case of interferences with the sulfur absorption (Fig. 5n–o). Spectra exhibit differences correlated to a different environment of lead atoms in the various compounds. The most striking difference between compounds with pure Pb(II) or mixed Pb(II)-Pb(IV) valence is the intensity of the pre-edge, which appears as a plateau for minium ( $\text{Pb}_3\text{O}_4$ ) and shows a more pronounced peak for the other compounds ( $\text{Pb}^{II}$ ). We have favored here the analysis of pigments similar to those used by painters. Preliminary simulations with the software FEFF [17] suggest that the plateau observed for  $\text{Pb}_3\text{O}_4$  results from the superposition of two shifted pre-edges, one at about  $2.488\text{ keV}$  for Pb(II) and  $2.492\text{ keV}$  for Pb(IV), for the  $M_V$ -edge. The atomic interpretation of these spectra requires additional analysis of pure references (litharge, massicot, plattnerite ( $\text{PbO}_2$ ), ...) and will be the subject of a dedicated article.

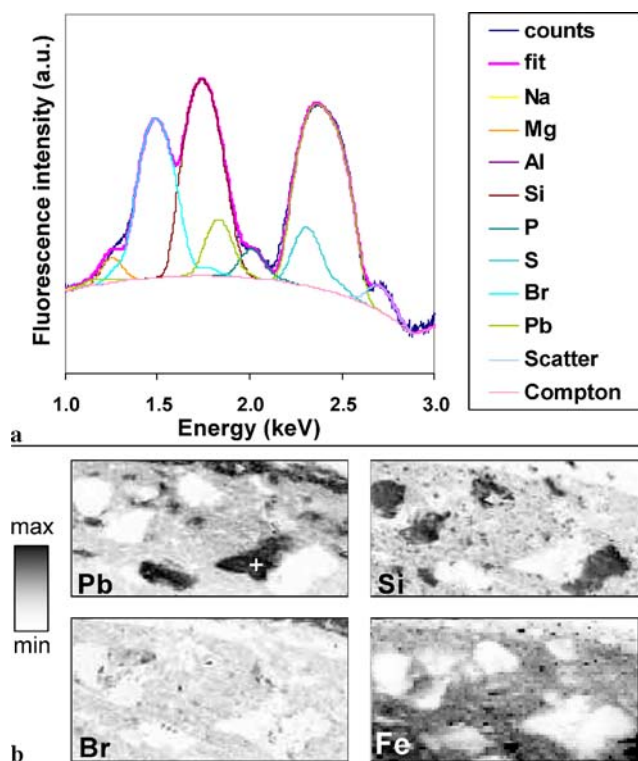


**FIGURE 4** Average micro-X-ray fluorescence spectrum obtained at 2.7 keV over the map and fitted with PyMCA (logarithmic scale) (a). Elemental mapping of Pb, Si, Br and Fe (b). Map size:  $450 \times 250 \mu\text{m}^2$ . The cross on the Pb-map indicates where the XANES spectrum presented in Fig. 5b was acquired

Spectra acquired in several points of the pellet were compared with references. The one obtained at the center of the lead soap protrusion is given as an example in Fig. 5b. Even if the spectral quality is not sufficient to clearly identify lead speciation, it is enough to resolve the pre-edges at 2.488 keV ( $M_V$ ) and 2.588 keV ( $M_{IV}$ ), which are in favor of Pb(II). Spectra, acquired in unfocussed mode over regions of about  $100 \mu\text{m}$  of various fragments from the painting confirm this observation.

In short, some hypotheses concerning the painter technique can be proposed. The painting is made of two main layers: the ground ochre layer and the colored layer, whose chemical composition and thickness are rather different.

The ground layer is a mixture of fat (presumably oil) and minerals. Oil is partially saponified by reaction with a lead compound, most probably Pb(II). The mineral is mainly composed of kaolinite and quartz: while the clay is intimately mixed to this organic paste, quartz appears as big particles of about  $50 \mu\text{m}$ -diameter. All these elements, in addition to the color and the presence of iron in the ground layer, are in agreement with the presence of ochre. Such a preparation has lots of similarities with a contemporaneous recipe, given by Sir Theodore Turquet de Mayerne in 1633 and describing the synthesis of lead media devoted to “impregnate canvas and avoid their splitting and their flaking” [18, 19]. Briefly, walnut oil is mixed with lead oxide (PbO), the liquid is then slightly heated. Afterwards, water is added, the temperature is increased and the mixture is stirred up to get a paste consistency. The first part of this recipe is a common way to prepare a basic

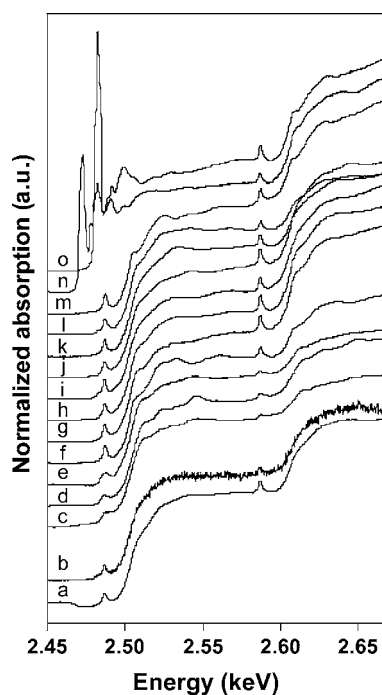


**FIGURE 5** Pb-XANES at the  $M_{IV}$  and  $M_V$  edges. Spectra acquired on the facsimile protrusion (cf. cross in Fig. 6CS.) (a), on the ancient painting protrusion (cf. cross in Fig. 4b-Pb) (b) and on various references: minium ( $\text{Pb}_3\text{O}_4$ ) (c), lead-tin yellow ( $\text{Pb}_2\text{SnO}_4$ ) (d), lead oxide (PbO) (commercial mixture of litharge and massicot) (e), cerussite ( $\text{PbCO}_3$ ) (f), phosgenite ( $\text{Pb}_2\text{CO}_3\text{Cl}_2$ ) (g), acetate ( $\text{Pb}(\text{C}_2\text{H}_3\text{O}_2)_2 \cdot 3\text{H}_2\text{O}$ ) (h), chloride ( $\text{PbCl}_2$ ) (i), laurionite ( $\text{PbOHCl}$ ) (j), palmitate ( $\text{Pb}(\text{C}_{16}\text{H}_{30}\text{O}_2)_2$ ) (k), lead white (commercial mixture of cerussite  $\text{PbCO}_3$ , and hydrocerussite  $\text{Pb}_3(\text{CO}_3)_2(\text{OH})_2$ ) (l), nitrate ( $\text{Pb}(\text{NO}_3)_2$ ) (m), galena (PbS) (n) and anglesite ( $\text{PbSO}_4$ ) (o)

lead-medium, famous for its siccativ properties [20, 21]. De Mayerne gives a last yet important indication: yellow ochre is added to this roasted oil (lead-medium) and the resulting paste can be directly applied on the canvas to impregnate it, before the application of colored layers.

Conversely, ochre is not detected in the superficial layer which confirms that the previous blend was specifically used for the ground layer and that the colored layer may have been prepared differently. The identification of lead white is not surprising as this pigment was extensively used, from the Antiquity up to the XX<sup>th</sup> century.

### 3.2 Synthesis of facsimile and model mixtures

The formation of lead soap protrusions is still poorly understood. It is sometimes described as the result of a long interaction between oil and lead compounds, in particular lead pigments [3–5]. Yet, the consideration of lead introduced as a siccativ (i.e. drier) and not as a pigment sheds different light on the saponification process. The reconstruction of ancient recipes mixing and curing oil and lead oxide has already been studied and shows the more or less rapid oil saponification. The kinetics are highly sensitive to the curing temperature and to the presence of water [2]. It demonstrates that this process enables obtaining of interesting mechanical properties as the resulting paste is more ductile than the original liquid oil. Indeed, the final product (lead-medium) is a mixture of unsaponified oil (liquid) and of lead soaps (solid

at room temperature) (see reference FTIR spectrum Fig. 7 spectrum (4)). In the case of the anonymous portrait studied here, experimental results agree with historical data, implying that the ground layer preparation is similar to De Mayerne's recipe. Yet, this preparation is given in order to get remarkable stability, and to prevent mechanical alterations of the painting, which is obviously not the case, considering the numerous cracking protrusions.

In order to better understand the evolution of such materials, a model lead-medium was prepared following De Mayerne's recipe [2]. Briefly, the paste was made with walnut oil, water and PbO, in the mass proportions 4 : 4 : 1. PbO was first mixed with oil, for 40 min at 60 °C. Then, boiled water was added and temperature was increased to 100 °C for 2 h, under constant stirring. The resulting paste was employed in two different ways. In one way, it was used to prepare a facsimile of the portrait. In other way, it was mixed with various pigments, among which there were lead-tin yellow, minium, lead white, raw umber and ochre, in order to follow the possible effect of pigments on ageing.

**3.2.1 Preparation and observation on the facsimile.** In brief, the ochre ground layer was obtained by mixing lead-medium with ochre and applied on a polyester canvas. Half this layer was left in contact with air (Fig. 6VL left), the other was covered with a brown colored layer, made of lead-medium mixed with azurite, vermilion and raw umber (Fig. 6VL right). Lead white pigment was intentionally excluded from this colored preparation in order to avoid an interfering additional supply of lead. After three months at room temperature, both parts of the facsimile exhibited a constellation of white protrusions (Fig. 6Z). Here again macro- and microscopic observations of these protrusions show that they grow inside the ground layer, and that they provoke the split of the superficial colored layer. Micro SR-FTIR and X-ray fluorescence analysis were performed on thin cross-sections, and revealed astonishing similarities to the original painting. The main results are summarized in Fig. 6. Unsurprisingly, the ochre thick under-layer is made of crushed kaolinite (Fig. 6k, Fe and Si), particles of quartz (Fig. 6q and Si) and partially saponified oil (Fig. 6u, f and Pb). As silicone is naturally present in both quartz and kaolinite, its distribution (Fig. 6Si) is the combination of the distribution of these two compounds (Fig. 6k and q). Lead was confirmed to be as the Pb(II) oxidation state (Fig. 5a). More interestingly, a high concentration of lead soaps is observed in the white-transparent protrusion (Fig. 6s and Pb) whereas unsaponified esters seem to be segregated on the protrusion border (Fig. 6u). The quality of both X-ray and FTIR spectra was highly improved thanks to the use of thin slices prepared with a microtome and the results are very similar to those obtained on the 17th century painting. It proves that the facsimile is an excellent model for this painting and supports De Mayerne recipes as a good equivalent of the one possibly used by the painter.

**3.2.2 Preparation and observation of the model mixtures lead medium-pigments.** Mixtures of lead-medium and pigments (lead-tin yellow, minium, lead white, raw umber and ochre) were applied on a glass slide and let dry at ambient temperature. The observations after one month showed the presence of

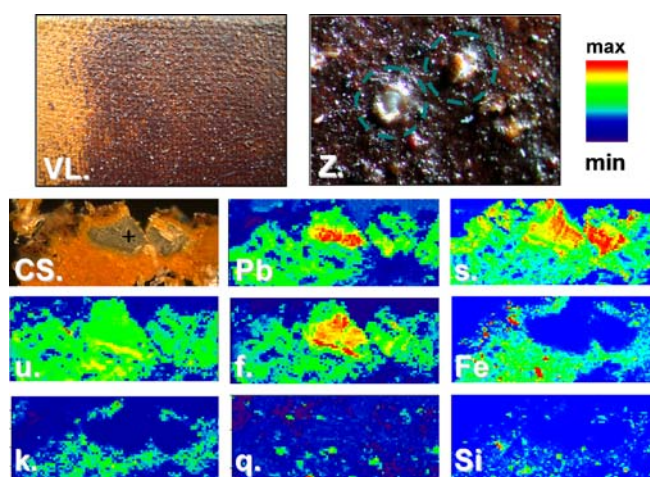


**FIGURE 6** Analysis of the facsimile. Visible light image (VL) showing both the ochre ground layer alone (left) and covered with the brown colored layer (right). Zoom on some white protrusions, after 3 months (Z), highlighted with green dotted circles. Visible light image of a 5  $\mu\text{m}$ -thick transversal cross section (CS), showing the white-transparent protrusion imaged by SR-FTIR and XRF. The cross indicates where the XANES spectrum presented in Fig. 5a was acquired. Chemical map of lead (SXM, Pb), carboxylates (FTIR, (s)), unsaponified groups (acids and esters) (FTIR, (u)), fatty chains  $\text{CH}_x$  (FTIR, (f)), iron (XRF, (Fe)), kaolinite (FTIR, (k)), quartz (FTIR, (q)) and silicon (XRF, (Si)). Map size: 550  $\times$  225  $\mu\text{m}^2$ ; step size: 5  $\mu\text{m}$  in both directions

some grains. These spots were analyzed by FTIR microscopy. In most of the cases, they were found to be pigment particles only, which were not sufficiently crushed and mixed with roasted oil. Conversely, an interesting observation was made on the mixture of lead-medium with lead white (referenced as "lw"). The main results are presented in Fig. 7. The map size is 0.94  $\times$  0.78  $\text{mm}^2$ , with the beam spot and the step size of 20  $\mu\text{m}$  in both directions. FTIR spectra are average of 64 scans. The visible light image shows two dark spots of about 80  $\mu\text{m}$  in a rather homogeneous light paste (Fig. 7VL). Spectra obtained in these two areas (Fig. 7 spectrum (1) and spectrum (2) respectively) are compared with the reference spectra of the original ingredients acquired before mixing and drying (lead white, Fig. 7 spectrum (3), and lead medium, spectrum (4)). Spectrum (2) of Fig. 7 is more or less representative of the superimposed contribution of lead-medium and of lead white. The main difference is the disappearance of the unsaturated C=C-H stretching signal at 3009  $\text{cm}^{-1}$ , which is a clear marker of drying and polymerization processes [14].

The spectrum (1) of Fig. 7 obtained on a dark spot is completely different. The signal of esters (1730  $\text{cm}^{-1}$ ) is highly reduced compared to that of original lead-medium which means that the saponification dramatically continued at this location. Indeed, the chemical maps of esters (Fig. 7e) and of soaps (Fig. 7s) confirm the local accumulation of carboxylates.

The profile of lead white (Fig. 7lw) was obtained by measuring the intensity of the absorption between 3600 and 3480  $\text{cm}^{-1}$ . It clearly shows that the black spots do not correspond to a local grain of pigment, as observed with other mixtures.

Even more interesting is the shape of the FTIR spectrum obtained in the dark spots, in the  $\text{CH}_2$  wagging and twisting-rocking vibrations domain (inset Fig. 7). As it was observed in the four-century-old anonymous portrait, the palmitic chain

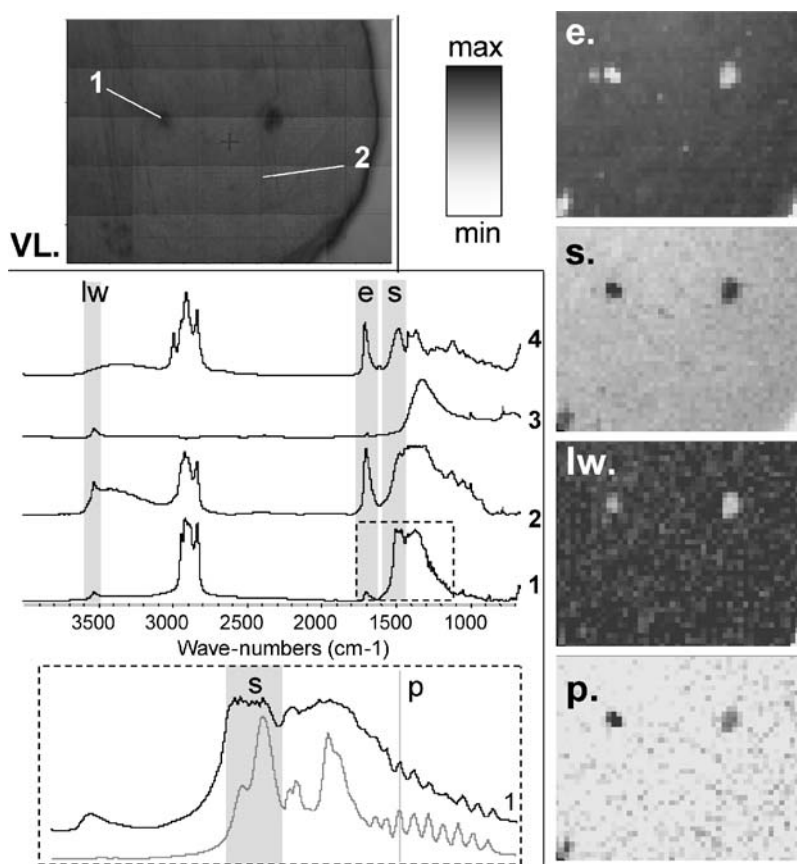


**FIGURE 7** Mixture of lead-medium and lead white, analyzed after 1 month by FTIR microscopy. Visible light image (VL). FTIR spectra acquired on a black spot (spectrum (1)), on the white matrix (spectrum (2)), on pure lead white (spectrum (3)) and on original lead-medium (spectrum (4)). In the *inset*, a zoom from 1800 to 1150  $\text{cm}^{-1}$  of spectrum (1) (*black*) is compared with reference spectrum of lead palmitate (*grey*). Chemical maps of esters (intensity from 1810 to 1651  $\text{cm}^{-1}$ ) (e), carboxylates (intensity from 1594 to 1485  $\text{cm}^{-1}$ ) (s), lead white (intensity from 3598 to 3479  $\text{cm}^{-1}$ ) (lw) and palmitic chains (intensity at 1295  $\text{cm}^{-1}$ , with a baseline from 1305 to 1285  $\text{cm}^{-1}$ ) (p)

signal is resolved. This fact does not automatically mean that the sample is made of pure crystallized palmitic chain. Other disordered chains may be present and contribute to the background signal. Nevertheless, it can be concluded that some palmitic chains are locally organized. This conformational order is restricted to the black spots (Fig. 7p).

The kinetics of formation and crystallization of these protrusions remains a controversial subject. Lead palmitates have already been observed in other paintings [3, 22], as well as in ancient cosmetics [1]. Information presented here demonstrates that crystallized lead soap aggregates can be formed after only one month and that, contrary to what can sometimes be found, protrusions formation does not necessarily require centuries. Lots of experiments have already been done to try to determine conditions that could favor oil saponification as well as lead soap protrusions [2, 3, 14, 23, 24]. Data are not easy to compare as various parameters are involved in the process: the choice of oil, of pigment, ageing conditions (moisture, temperature) that may change from one study to another.

Lead white is rather a special pigment which can exhibit different behaviors toward saponification. This pigment is often found as a mixture of lead carbonate (cerussite  $\text{PbCO}_3$ ) and lead hydroxy-carbonate (hydrocerussite,  $\text{Pb}_3(\text{CO}_3)_2(\text{OH})_2$ ). Several mixtures of linseed oil and lead white, mimicking painting preparations, allow the formation of carboxylates after a more or less long time [3, 14, 23, 24]. On the contrary, pure cerussite has shown a very low ability to saponification, even in drastic conditions [2]. This difference is certainly due to the fact that hydrocerussite is far more ba-

sic than cerussite, hence lead white has a greater capacity to saponification than pure cerussite.

#### 4 Conclusion

This work provides a different insight into the general study of lead soap protrusions. The technical and methodological approaches used here were found to be rather powerful for gaining access to chemical information. Lead involved in protrusions does not necessarily come from pigment, but more presumably from siccative, as was proved with the facsimile. Lead soap aggregates formation, and crystallization does not necessarily require centuries but can be observed after a few weeks, as it was the case in both the facsimile, and the model mixtures.

These preliminary results are only a part of a more general understanding of the mechanism describing the protrusions phenomenon. Lots of questions are still open: what does promote the crystallization of lead soaps, and in particular lead palmitates? Is there any chain segregation and how? Why are some protrusions orange whereas others are white? One hypothesis we propose is that lead soap aggregates are due to a local source of lead oxide and its local reaction with oil. In fact, during the preparation of a lead-medium by mixing oil with lead oxide, saponification is not complete. Some unsaponified esters remain, which provide the flexibility of the final product. It can be supposed that, if lead oxide is not sufficiently ground, particles may remain in the lead-medium, supplying a local source of reactive lead oxide. A major parameter, which is in fact often underlined in ancient texts, is

the size of lead oxide grains, and the attention paid to grinding. These hypotheses must be confirmed by another set of experiments. A complete understanding of protrusions formation will require a detailed study of the physical properties (diffusion and structural organization) in addition to chemical analysis.

**ACKNOWLEDGEMENTS** The authors thank JL Coudrot, Head conservator of the Musée du Châtillonnais, for its kind authorisation to publish the picture of the anonymous portrait, and the reviewers for their careful readings of the manuscript, and for their constructive remarks.

## REFERENCES

- 1 M. Cotte, P. Dumas, G. Richard, R. Breniaux, P. Walter, *Anal. Chim. Acta* **553**, 105 (2005)
- 2 M. Cotte, E. Checroun, J. Susini, P. Dumas, P. Tchoreloff, M. Besnard, P. Walter, *Talanta* **70**, 1136 (2006)
- 3 C. Higgitt, M. Spring, D. Saunders, *Nat. Gallery Technol. Bull.* **24**, 75 (2003)
- 4 K. Keune, J.J. Boon, *Anal. Chem.* **76**, 1374 (2004)
- 5 G. Chiavari, D. Fabbri, S. Prati, *J. Anal. Appl. Pyrol.* **74**, 39 (2005)
- 6 J.-S. Tsang, R.H. Cunningham, *J. Am. Inst. Conserv.* **30**, 163 (1991)
- 7 M. Derrick, L. Souza, T. Kieslich, H. Florsheim, D. Stulik, *J. Am. Inst. Conserv.* **33**, 227 (1994)
- 8 M.R. Derrick, D. Stulik, J.M. Landry, *Scientific Tools for Conservation, Infrared Spectroscopy in Conservation Science* (The Getty Conservation Institute, Los Angeles, CA, 1999)
- 9 J. van der Weerd, *Microspectroscopic Analysis of Traditional Oil Paint* (Thesis, Amsterdam, 2002), downloadable from <http://www.amolf.nl/publications>
- 10 J. Susini, M. Cotte, K. Scheidt, O. Chubar, F. Polack, P. Dumas, SRN, to be published
- 11 J. Susini, M. Salomé, B. Fayard, R. Ortega, B. Kaulich, *Surf. Rev. Lett.* **9**, 203 (2002)
- 12 V.A. Solé, E. Papillon, M. Cotte, Ph. Walter, J. Susini, *Spectrochim. Acta, Part B* **62**, 63 (2007)
- 13 E. Welcomme, P. Walter, E. van Eslande, G. Tsoucaris, *Appl. Phys. A* **83**, 551 (2006)
- 14 R.J. Meilunas, J.G. Bentsen, A. Steinberg, *Stud. Conserv.* **35**, 33 (1990)
- 15 D. Chapman, *The Structure of Lipids by Spectroscopic and X-ray Techniques* (Spottiswood, Ballantyne and Co Ltd., London and Colchester, 1965)
- 16 L. Robinet, M.C. Corbeil, *Stud. Conserv.* **48**, 23 (2003)
- 17 A.L. Ankundinov, B. Ravel, J.J. Rehr, Manual of the FEF8.10 program. The FEF8 Project (Univ. of Washington, Seattle, USA, 2000)
- 18 Theodore Turquet De Mayerne, *Pictoria, Sculptoria, Tinctoria, et quae subalternarum artium* (Manuscript) (British Museum London, Ms. Sloane 2052), pp. 1620–1642
- 19 M. Faidutti, C. Versini, *Le manuscrit de Turquet de Mayerne présenté par M. Faidutti et C. Versini* (shortened edition) (Lyon, 1965)
- 20 L. Carlyle, *J. Am. Inst. Conserv.* **38**, 69 (1999)
- 21 R. White, J. Kirby, *Nat. Gallery Technol. Bull.* **15**, 64 (1994)
- 22 M.J. Plater, B. De Silva, T. Gelbrich, M.B. Hursthouse, C.L. Higgitt, D.R. Saunders, *Polyhedron* **22**, 3171 (2003)
- 23 J. van der Weerd, A. van Loon, J.J. Boon, *Stud. Conserv.* **50**, 3 (2005)
- 24 R. Arbizzani, U. Casellato, E. Fiorin, L. Nodari, U. Russo, P.A. Vigato, *J. Cult. Herit.* **5**, 167 (2004)